Journal of Thermal Analysis and Calorimetry (2023) 148:13107–13119
https://doi.org/10.1007/s10973-023-12525-2

Thermal stabilization of recycled PLA for 3D printing by addition of charcoal

Daniela Fico[1] · Carola Esposito Corcione[1] · Maria Rosaria Acocella[2] · Daniela Rizzo[3] · Valentina De Carolis[1] · Alfonso Maffezzoli[1]

Received: 22 June 2023 / Accepted: 19 August 2023 / Published online: 15 September 2023

Abstract

Poly(lactic acid) (PLA) is one of the most widely used thermoplastic materials for 3D printing, particularly in the Fused Filament Fabrication technique. However, the printing process generates waste products and even though PLA is compostable, the possibility of recycling it provides ecological and economical benefits. In this work, a study on the stabilization of recycled PLA using charcoal (CC) was carried out, with the aim of overcoming the well-known problem of degradation (reduction in molecular weight) of PLA, during remelting. Microscopic investigations showed good dispersion of the filler in the polymer matrix, as well as better adhesion between the printed layers. Thermal analyses (Differential scanning calorimetry and thermogravimetry) indicate a stabilization of PLA waste because of the addition of small concentrations of CC to the recycled polymer matrix. These data are confirmed by GPC analyses, which show that the addition of filler is associated with higher molecular weight. Mechanical analysis indicated improved elongation at break and elasticity. Finally, a key ring was printed as an example of the better printability of the filament containing CC. The results indicate that a stabilization of the recycled PLA with a very low concentration of CC has been achieved. Improved 3D printability and properties of the 3D printed objects can be attained through recycling and recovery of wasted PLA, according to sustainability and circular economy matters.

Keywords Poly(lactic acid) · Waste recycling · Circular economy · Bio-composite · 3D printing

Introduction

In recent years, along with the increase of plastics use, the problem of persistent and harmful waste in the environment has also increased. Therefore, the issues related to the environmental impact of plastics and their disposal methods have become increasingly important, leading to more restrictive worldwide legislations [1–3]. The possibility of substituting oil-derived plastics with biodegradable or bio-based polymers as well as bio-composite materials has attracted scholars and researchers. Several scientific researchers recently focused on the development of green and sustainable polymer based materials [4–7]. Among these, the wide range of commercially available biopolymers, to be used as matrix for composites has noticeably increased [8–11]. The features of bio composites suggest their possible use in several industrial sectors, such as food, pharmaceutical, medical, aerospace, automotive, architectural, artistic, textile, etc., as well as for the production of everyday objects [12]. However, even if they are sustainable or natural materials, the end of life of all these materials still

✉ Carola Esposito Corcione
carola.corcione@unisalento.it

Daniela Fico
daniela.fico@unisalento.it

Maria Rosaria Acocella
macocella@unisa.it

Daniela Rizzo
daniela.rizzo@unisalento.it

Valentina De Carolis
valentina.decarolis@unisalento.it

Alfonso Maffezzoli
alfonso.maffezzoli@unisalento.it

[1] Department of Engineering for Innovation, University of Salento, Edificio P, Campus Ecotekne, S.P. 6 Lecce-Monteroni, 73100 Lecce, LE, Italy

[2] Department of Chemistry and Biology, University of Salerno, Via Giovanni Paolo II 132, 84084 Fisciano, SA, Italy

[3] Department of Cultural Heritage, University of Salento, Via D. Birago 64, 73100 Lecce, LE, Italy

causes an increase in the volume of waste. The latter issue has prompted researchers to investigate new ways of recycling, transforming and valorizing biopolymers and bio composites, too. In fact, the possibility of reusing materials allows to give them a second life, resulting in new consumable products and ecological and economic benefits. These principles are the basis of the Circular Economy (CE) and Sustainable Development, and constitute a concrete answer to environmental and social problems, overcoming the linear model, used until now [13]. The large-scale diffusion of Additive Manufacturing (AM) technologies, or so-called 3D printing, including Fused Filament Fabrication (FFF), has also increased the use of these technologies in the CE [12, 14]. Specifically, the advent of FFF printing and its diffusion on the market (both at an industrial and do-it-yourself level), has changed the way of producing 3D objects, through a layered production process. The latter method presents several advantages compared to the traditional processing methods, such as savings in raw materials, easy personalization of the product, decreasing of the production costs and time to market [15–17]. For all these reasons, the FFF printing market is nowadays a strong growth sector. The traditional filaments used in FFF printing are thermoplastic polymers, such as poly(lactic acid) (PLA), acrylonitrile butadiene styrene, polycaprolactone, poly-carbonate, various types of polyethylene, of different densities [12, 18–20]. Composites and nano-composites [21–25], made of naturally derived and biodegradable and/or sustainable materials, even obtained from waste recycling [8, 12, 26–32], are also used. However, despite its numerous advantages, FFF printing generates large quantities of waste, which are the result of failed prints, unsuitable aesthetic prototypes and discarded support structures [29, 33]. In order to overcome this limit, in recent years, research has focused on the production of filaments for FFF from recycled polymers. Among these, PLA is, at the same time, the most widely used thermoplastic polymer in 3D printing and the most used biopolymer [34]. It is a bio-based and bio-compostable polymer [35], which is obtained from lactic acid monomers, produced from natural renewable resources, such as wheat, maize and industrial or agricultural waste by fermentation [12, 36]. Although it is sensitive to water and high temperatures (around 200 °C), the biodegradability time of pure PLA ranged between 30 and 180 days under extreme environmental conditions, but this period increases in presence of fillers, dyes and plasticizers [3, 37–40]. Already in 2017, Anderson [41] made an initial attempt to recycle printed PLA, obtaining similar mechanical properties for the neat and recycled 3D printed models. Gil Muñoz et al. [34] developed novel PLA filaments from the waste of FFF prints, produced both by the University of Madrid (Spain) and by makers of personal protective equipment during the Covid-19 pandemic [34]. Lanzotti et al. [42] compared the mechanical properties of 3D objects, printed by using both virgin and recycled poly(lactic acid) (PLA), showing a decay in properties and greater variability as the number of filament re-extrusion cycles increased [42]. Beltrán et al. [33] showed higher biodegradability, crystallinity and lower intrinsic viscosity of recycled PLA samples, especially in the sample obtained by combining different PLA scraps. Zhao et al. [43] showed a significant degradation of PLA due to the recycling process. Or again, Beltran et al. [33] report a decrease in the molecular weight of PLA recycled from 3D prints, as a consequence of the presence of shorter polymer chains. M.E. Grigora et al. [44] examined the effect of the chain extender named Joncryl ADR® 4400 on the physic-chemical properties and printability of PLA, demonstrating an increase in molecular weight and viscosity. Despite its stabilizing effect, the reaction typically involves the epoxy groups in the chain extender, providing branching points in the matrix that, when chemically bonded, produce structural disorder inhibiting matrix nucleation. Furthermore, chain extenders would change wire extrusion in a reactive process, making it more complex and not easily controllable.

For these reasons, scientific research is moving towards the development of new sustainable strategies that can improve PLA recycling. Fico et al. [29] in a recent paper proposed a hand-made and low-cost strategy of using 100% recycled PLA filament for the creation of supports and fillings of printed objects. Even though the authors highlight a significant deterioration of mechanical properties due to recycling, they support the possibility of using it for non-structural purposes in the FFF technique, still obtaining economic and ecological benefits [29]. Instead, Beltrán et al. [33] proposed a solid-state polymerisation process to increase the molecular weight of recycled PLA [33]. D'Urso et al. [45] demonstrated the good effect of high surface area graphite and carbon black on the degradation of PLA during melting [45]. Moreover, D'Urso et al. [46] showed that alkylated carbon black) added to the polymer matrix in PLA not only induces a high thermal stabilization of the melt, but also acts as a nucleating agent, thus reducing crystallization time [46]. In this framework, the role of a charcoal (*Carbo lignis pulveratus)* obtained as a product from natural source, as a melt-stabilizing agent of PLA recycled from FFF-produced prints was investigated. The main purpose of the study is to propose a method to overcome the well-known problem of molecular weight reduction of PLA in the melt state, occurring also in 3D printing by FFF. This degradation makes critical the recycling of PLA in FFF and weak and brittle the obtained parts.

Materials and methods

The study on the reprocessability of poly(lactic acid) (PLA) through the addition of a natural filler (CC), as a stabilizing agent, was carried out by comparing the morphological,

thermal and structural properties of the neat materials, the FFF filaments and the respective 3D printed models. The following sections provide details on the raw materials, the production and analysis methods.

Materials

The neat materials used in this work are listed in Table 1. Charcoal, *Carbo lignis pulveratus*, (CC) was purchased from Caesar & Loretz GmbH (Hilden, Germany). Its Oxygen/Carbon weight ratio, as evaluated by elemental analysis, was high (O/C = 0.29) and was used as filler to produce the composite filament. The poly(lactic acid) waste used for the production of the recycled filaments was derived from unusable FFF printed parts (i.e. supports, test prototypes, failed print, etc.). The PLA filaments of different colors (diameter 1.75 ± 0.02 mm) were purchased from the company Sunlu (Guangdong, China) and used to produce the 3D prints. The names of the raw materials used (PLA pellets and Sunlu PLA filament) and the unused pieces of different coloured prints (PLAW) are shown in Table 1. According to the manufacturer's data sheet, Sunlu PLA filaments are characterized by a density of 1.24 g cm^{-3}, a melt flow index (MFI) of 7–9 g/10 min at a temperature of 190 °C. Before using, the waste materials were washed with tap water and then dried in an oven at 60 °C until constant weight is reached. Then, the recycled prints were reduced to powders of a mean size of 0.75 mm, using first the SM100 cutting mill and then ZM 100 Ultra Centrifugal Mill (Retzsch GmbH, Haan, Germany).

Production of filament for FFF

Two recycled filaments for FFF printing were developed. The first, made of 100 mass% of PLA waste and labelled PLAR_f, was produced by mixing all PLA waste microfragments, labeled PLAWt, PLAWw, PLAWb, PLAWr, PLAWbk. The second consisted of 97.5 mass% of recycled PLA and 2.5 mass% of CC and it is labelled PLAR/CC_f (Table 2).

Table 1 Neat materials labels and weight composition/mass%

Label	Composition/mass%
PLA	PLA pellet
PLA Sunlu	PLA Sunlu filament
PLAWt	Recycled PLA Sunlu transparent
PLAWw	Recycled PLA Sunlu white
PLAWb	Recycled PLA Sunlu blue
PLAWr	Recycled PLA Sunlu red
PLAWbk	Recycled PLA Sunlu black
CC	Charcoal

To produce the composite filament, PLA powder (0.75 mm), obtained starting from the different PLA waste (Table 1), and CC particles with a size in the 5–60 μm, were first mixed manually at room temperature and then fed to the extruder. Extrusion of the filaments was carried out with the 3Devo Composer 450 Filament Maker single-screw extruder (Utrecht, The Netherlands), using the parameters shown in Table 3.

3D printing

The FFF recycled filaments shown in Table 2 (PLAR_f and PLAR/CC_f) were used for bars fabrication (labelled as PLAR_3D and PLAR/CC_3D, respectively). Specifically, bars of dimensions 80 mm × 10 mm × 4 mm were printed using the Creality CP-01 printer (Creality, London, UK), in accordance with the European Standard ISO178:2014. The following operating conditions were used: extrusion temperature 200 °C, plate temperature 50 °C, printing speed 50 mm/s, infill 100%. The CAD model was created with Fusion 360 software (Autodesk, San Rafael, CA, USA), which was converted to an GCode file, using Cura software (Ultimaker B.V., Utrecht, The Netherlands). Finally, after testing the morphological and mechanical properties of the printed bars, as an example of the better printability of the biocomposite filament, a key ring was printed using the same printing machine and the following operating parameters: extrusion temperature 200 °C, plate temperature 50 °C, printing speed 50 mm/s, infill 20%. The CAD model was created with Fusion 360 software (Autodesk, San Rafael, CA, USA), which was converted to an GCode file, using Cura software (Ultimaker B.V., Utrecht, The Netherlands).

Table 2 Recycled filament labels and weight composition/mass%

Sample	Label	Composition/mass%
Recycled filament for FFF	PLAR_f	Recycled PLA Sunlu (100)
	PLAR/CC_f	Recycled PLA Sunlu (97.5)/Charcoal (2.5)

Table 3 Extrusion process parameters for filaments

Extrusion process parameters	PLAR_f	PLAR/CC_f
Screw speed /rpm	4	3.5
Feed zone temperature /°C	195	175
Compression zone temperature /°C	190	190
Metering zone temperature /°C	190	185
Die temperature /°C	200	170

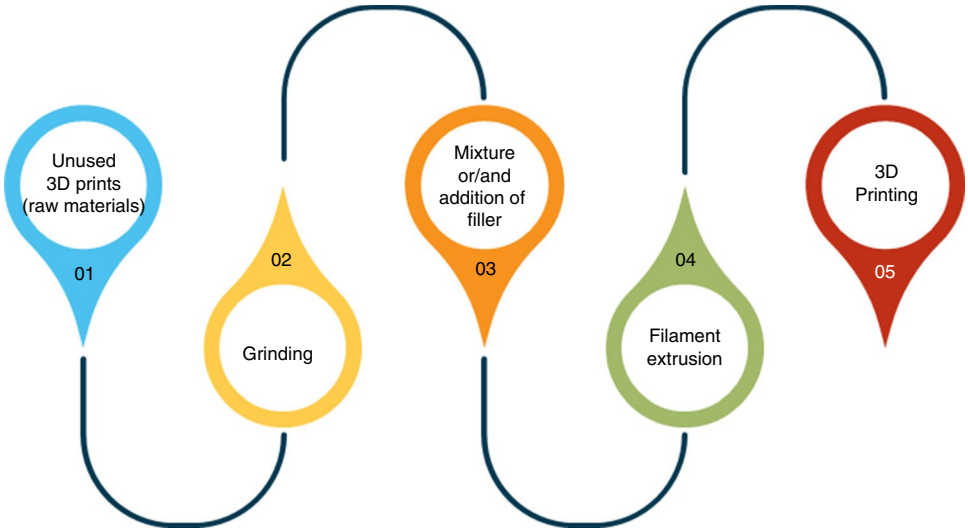

Fig. 1 Diagram of the process steps of the different samples

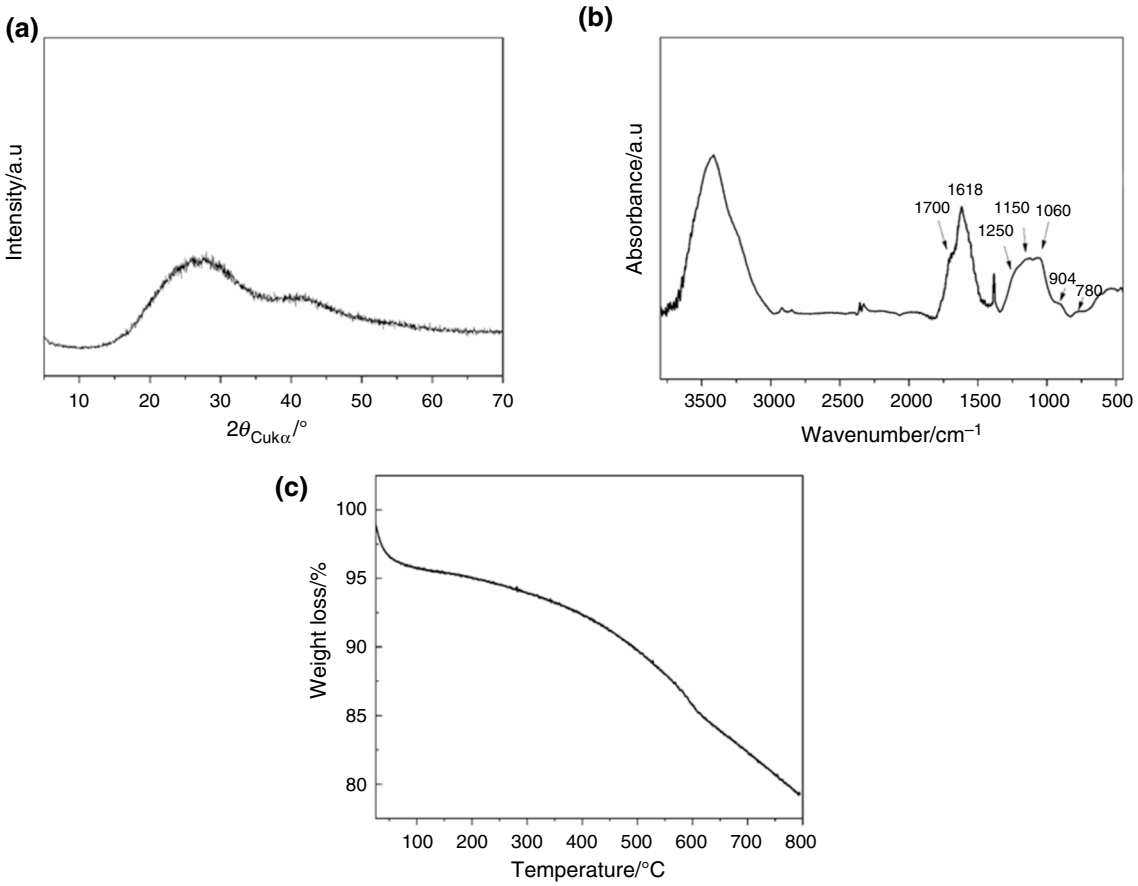

Fig. 2 RX-diffraction pattern **a**, FTIR spectra **b** and TGA scan **c** of Charcoal

The production process of the 3D printed models consisted in five steps, responsible of different melting/solidification cycles of the recycled PLA, as shown in Fig. 1.

Methods

Elemental analyses of charcoal were performed with a Thermo FlashEA 1112 Series CHNS-O analyzer by Thermo

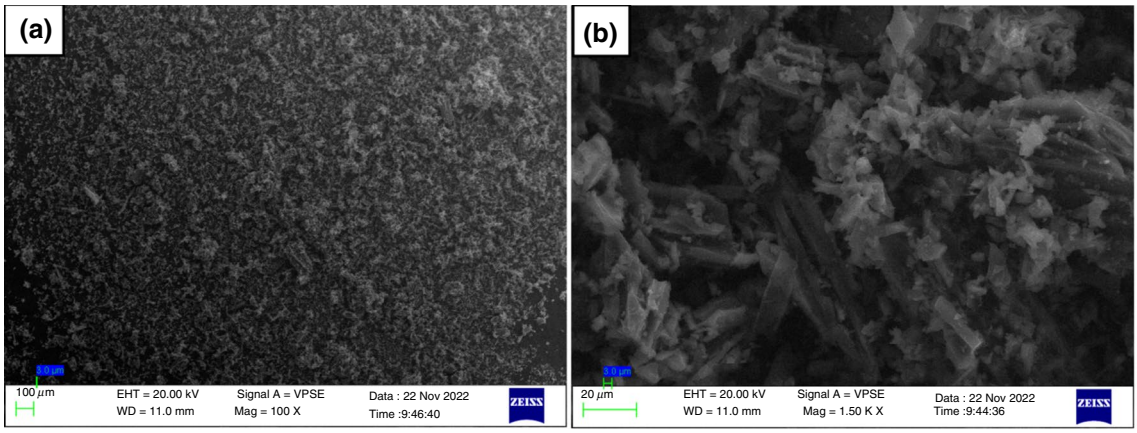

Fig. 3 SEM images of filler CC: **a** magnification 100x, **b** magnification 1500x

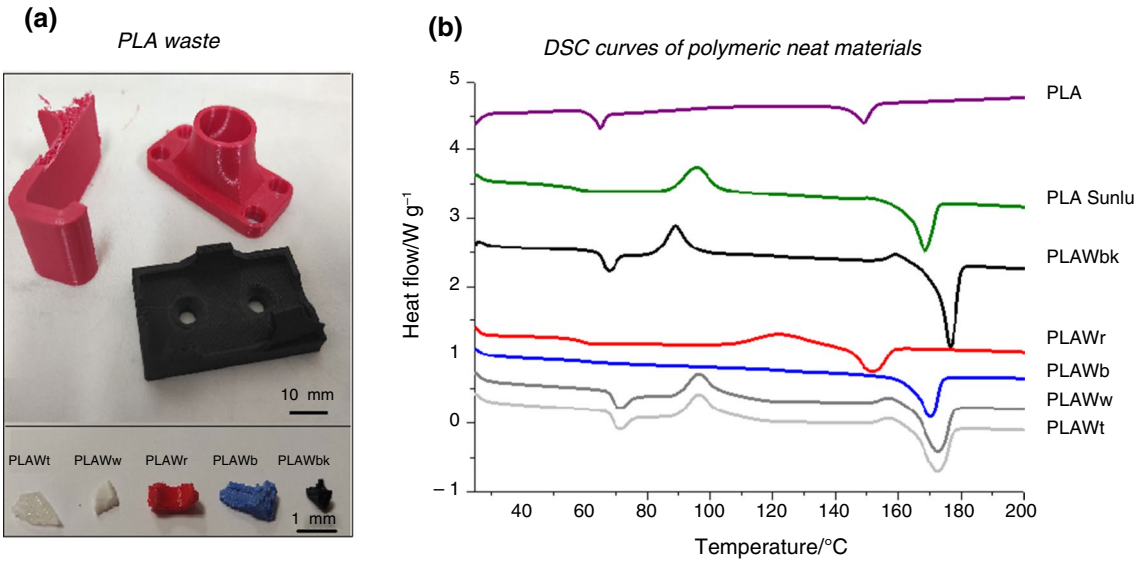

Fig. 4 **a** PLA waste; **b** DSC curves of polymeric neat materials

Fisher Scientific Inc. (Waltham, MA, USA), after pre-treating CC samples in an oven at 100 °C for 12 h.

Surface areas of CC were measured by nitrogen adsorption at liquid nitrogen temperature (77 K) with a Nova Quantachrome 4200e instrument by Quantachrome Instruments (Boynton Beach, FL, USA). Before adsorption measurements, samples were degassed at 80 °C under vacuum for 24 h. The surface area (SA_{BET}) value was determined by using 11-point Brunauer-Emmett-Teller (BET) analysis.

Wide-angle X-ray diffraction (WAXD) patterns were obtained for CC in reflection, at 35 kV and 40 mA, using the nickel filtered Cu-Kα radiation (1.5418 Å), by an automatic Bruker D8 Advance diffractometer (Karlsruhe, Germany).

Table 4 Thermal properties obtained from DSC analysis of polymeric neat materials: glass transition temperature (T_g), temperature and enthalpy of crystallization (T_c and ΔH_c) and melting temperature and enthalpy (T_m and ΔH_m)

Sample	T_g /°C	T_c /°C	ΔH_c /J g^{-1}	T_m /°C	ΔH_m /J g^{-1}
PLA	60.0	–	–	153.6	19.9
PLA Sunlu	68.7	96.3	23.4	172.6	30.9
PLAWt	68.8	96.2	23.4	172.4	31.9
PLAWw	68.3	95.9	23.5	172.7	30.7
PLAWb	60.1	–	–	170.2	25.6
PLAWr	58.9	121.7	16.3	151.7	20.8
PLAWbk	65.8	88.7	20.4	176.8	42.9

XRD analysis (Rigaku Ultima + Tokyo, japan) was performed on PLA pellet and recycled filaments with CuKα radiation (λ = 1.5418 Å) in the step scan mode recorded in the 2θ range of 2°–60°, with a step size of 0.02° and a step duration of 0.5 s.

Thermogravimetric analysis (TGA) was carried out on the waste materials (CC and PLA waste) and filaments using Q500 equipment manufactured by TA Instruments, from 20 to 800 °C at a heating rate of 10 °C under N_2 flow. Samples were pretreated in an oven at 100 °C for 12 h, in order to remove the absorbed water.

FTIR spectra of charcoal were obtained at a resolution of 2.0 cm^{-1} with a FTIR spectrometer (Bruker Vertex70, Bruker, Karlsruhe, Germany) equipped with deuterated triglycine sulfate (DTGS) detector and a KBr beam splitter, using KBr pellets. The frequency scale was internally calibrated to 0.01 cm^{-1} using a He–Ne laser. 32 scans were signal averaged to reduce the noise. Morphological analysis was performed on the charcoal and on the filaments to determine morphology and particle size and on the filaments with a Scanning Electron Microscope (SEM), model Zeiss E Evo 40 (Oberkochen, Germany).

Differential Scanning calorimetry (DSC) (Mettler Toledo DSC1 StareSystem) was performed on polymer raw materials, filaments and 3D printed bars, to assess the effect of the addition of the charcoal on the PLA recycling process, by measuring glass transition temperature (T_g), crystallization temperature (T_c) and melting temperature (T_m) of PLA. The analyses were conducted using a temperature range of 25 °C to 200 °C at a heating rate of 10 °C min^{-1}.

Gel permeation chromatography (GPC) measurements were conducted on the filaments by a Waters Breeze GPC system (Waters, Milford, MA, USA), equipped with a refractive index detector, by using a set consisting of four Styragel HT columns with 10^2, 10^3, 10^4, and 10^5 Å pore size and 10 µm of particle size. Tetrahydrofuran (THF) was used as eluent at 35 °C at a flow rate of 1.0 mL min^{-1}. The calibration curve was obtained by using polystyrene standards. Analyzed samples were dissolved in THF at 50 °C with a concentration of 1 mg ml^{-1}. The obtained solutions were then filtered by using a Chromafil PTFE 0.45 µm filter.

According to the ISO178(2014) standard, flexural tests were performed on 3D printed bars using a Lloyd LR50K dynamometer (Lloyd Instruments Ltd., Bognor Regis, UK), with a test speed of 2 mm min^{-1} and a specimen support spacing of 64 mm. Five replications were performed for each specimen.

Magnification images of the 3D printed bar sections were obtained using the Dino-Lite Digital Microscope instrument (AnMo Electronics Corporation, New Taipei City, Taiwan), to check the morphology and adhesion of the different deposited layers.

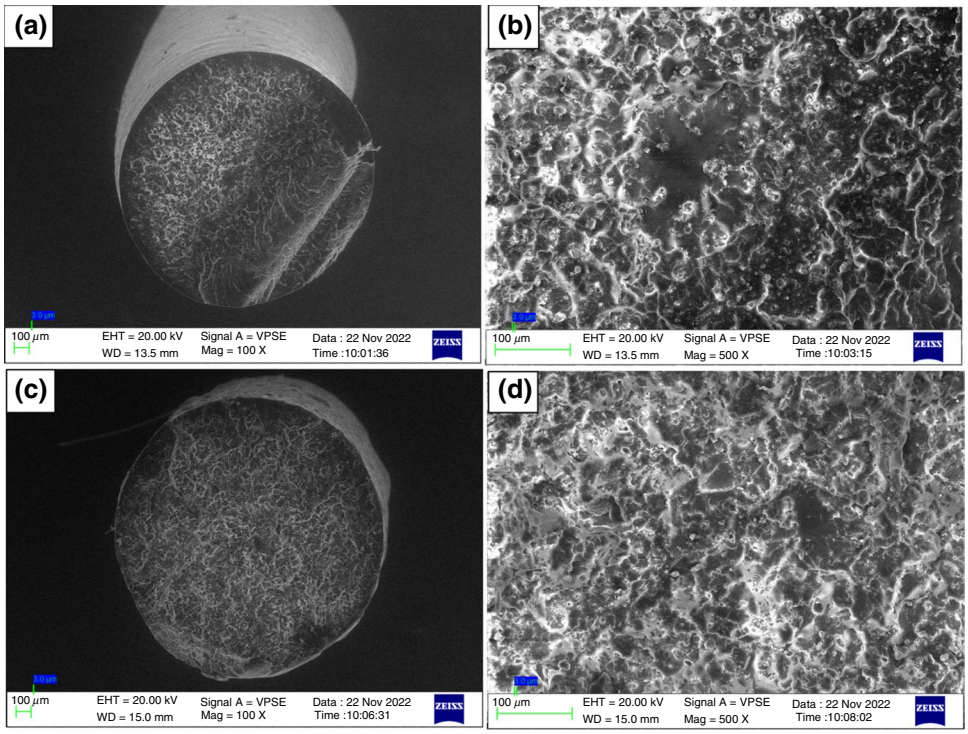

Fig. 5 SEM images of filaments: PLAR_f, magnification 100x (**a**) and 500x (**b**); PLAR/CC_f, magnification 100x © and 500x (**d**)

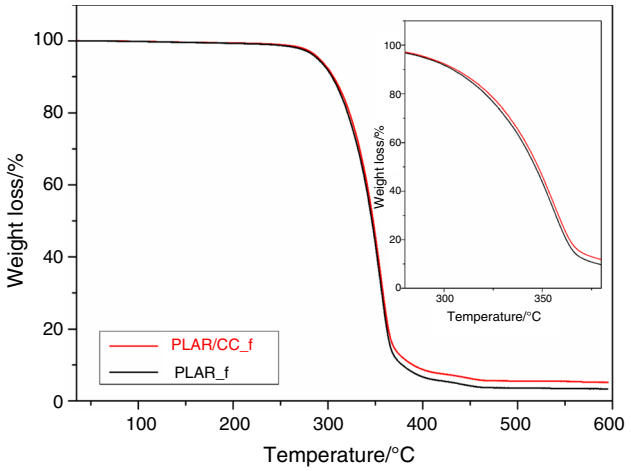

Fig. 6 TG scans for the PLA filament after 3D printing PLAR_f (black) and for PLA filament with 2.5 mass% of charcoal after 3D printing PLAR/CC_f (red)

Results and discussion

Characterization of neat materials

Charcoal

Charcol with an O/C ratio of 0.29, as evaluated by the elemental analysis and with $SA_{BET} = 50 m^2 g^{-1}$, was fully characterized by X-ray diffraction analysis, FTIR spectroscopy and Thermogravimetric analysis, as reported in Fig. 2a,b and c.

Specifically, the X-Ray diffraction pattern shows two very broad amorphous halos indicating the occurrence of a high degree of disorder in the spatial arrangement of defective small graphene layers, associated with its high oxygen content. The presence of many oxygenated functional groups is also confirmed by FTIR spectrum. The charcoal shows well-defined peaks at 1700 and 1618 cm^{-1} related to unsaturated ketones and lactones [47] and C=C stretching vibration, respectively. Moreover, broad bands at 1250, 1150 and 1060 cm^{-1} reveal the contribution of vinyl ether and secondary alcohol, while 904 and 780 cm^{-1} peaks can be assigned to asymmetric stretching and deformation vibrations of epoxy groups [48], respectively. TGA scans of charcoal shown in Fig. 2c, also exhibits the usual behavior due to the degradation of oxygenated functionalities [49]. More interestingly, the SEM images of the filler (Fig. 3a and b) reveal particles aggregates possibly resulting from lignin degradation embedding cellulose microfibrils residue originating from the pyrolysis of cellulose, hemicellulose, and lignin, the typical biomass constituents. Micropores are instead not visible, confirming the low surface area detected by specific SA_{BET} measurement.

PLA waste

The DSC curves of PLA pellet, filament and of different PLA waste (Fig. 4a) are shown in Fig. 4b. They appear very different from each other, and this is probably due to the presence of additives, plasticizers and dyes, typically used

Table 5 Thermal properties obtained from DSC analysis of recycled filaments glass transition temperature (T_g), temperature and enthalpy of crystallization (T_c and ΔH_c) and melting temperature and enthalpy (T_m and ΔH_m)

Sample	T_g /°C	T_c /°C	ΔH_c /J g^{-1}	T_m /°C	ΔH_m /J g^{-1}
PLAR_f	57.3	95.5	22.1	168.1	24.5
PLAR/CC_f	58.9	91.9	27.8	167.0	34.7

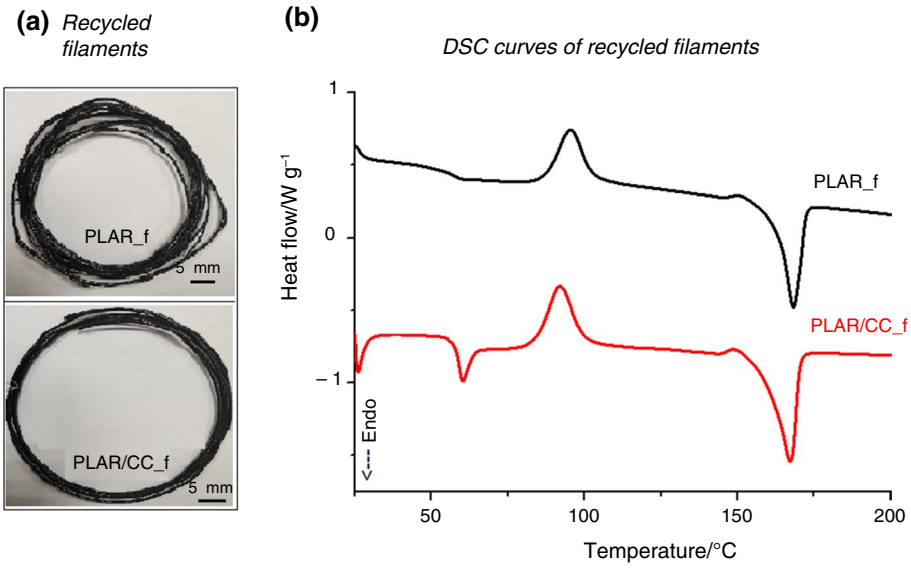

Fig. 7 **a** Recycled filaments; **b** DSC curves of recycled filaments

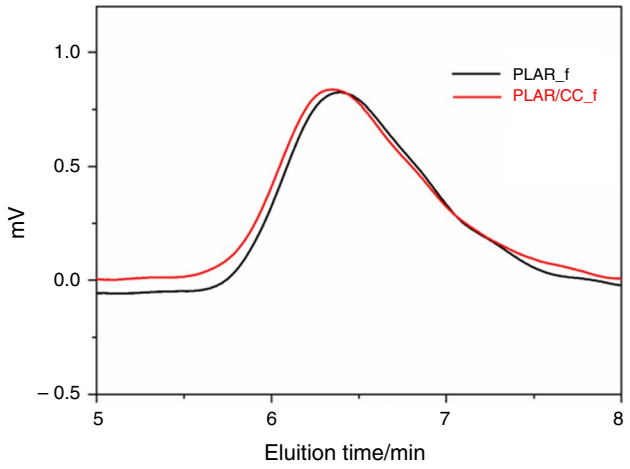

Fig. 8 GPC curves of the recycled filaments

Table 6 Number average molecular weight (M_n), weight average molecular weight (M_w) and polydispersity index (PDI) as evaluated by GPC curves, for samples with and without charcoal. The evaluated variance is of ± 3 kDa

Label	M_n /g mol^{-1}	M_w /g mol^{-1}	PDI
PLA	106,418	209,921	1,97
PLA_f	58,569	142,096	2,42
PLAR_f	17,436	57,433	3,29
PLAR/CC_f	21,982	64,677	2,94

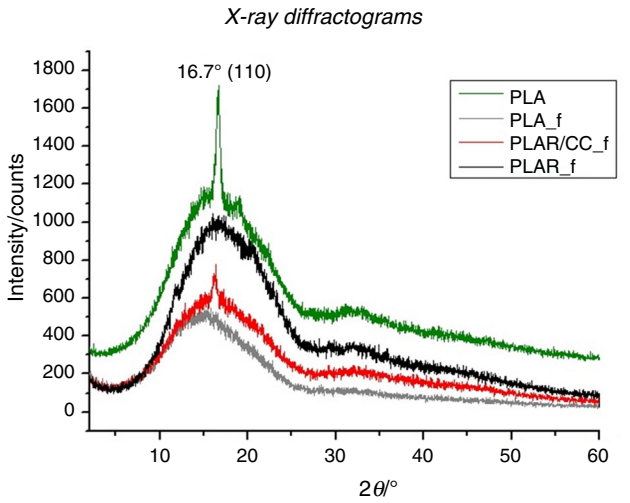

Fig. 9 X-ray diffrattograms of PLA, PLA_f and recycled filaments PLAR/CC_f and PLAR_f

in commercial filaments, even if they are not always reported in the manufacturer's data sheets. The glass transition temperatures (T_g) of all recycled materials were measured using the inflection point method. The measured values are shown in Table 4. It is evident that PLA, PLAWr and PLAWb show similar T_g values, also comparable to that reported in the literature for PLA [12, 26, 28]. On the other hand, higher T_g values were measured for PLA Sunlu, PLAWw, PLAt, PLAbk samples, probably due their slightly different composition. Furthermore, for the latter, the glass transition is accompanied by a an endothermic peak (relaxation enthalpy) due to the transformation of the polymer from the glassy to the liquid-viscous or rubbery state [50–52]. The absence of cold crystallization is observed in the DSC curves of the PLA and PLAWb sample. In contrast, the other PLA filament and waste shows cold crystallization temperatures (T_c) ranging from 95.9 °C to 121.7 °C (Fig. 4b). The melting temperature (T_m) ranges between 151.7 °C and 176.8 °C. As expected, the results obtained from the thermal analysis confirm the heterogeneity of filaments even though they are produced by the same company. All the discarded prints reported in Table 1 were used to produce the recycled filaments for FFF with the aim of simulating typical home-made conditions and trying to overcome the problems of different processability and polymer degradation, that is most evident when mixing PLA of different origin.

Characterization of Filaments for FFF

SEM analyses were performed on the fracture sections of the two produced filaments and reported in Fig. 5a–d. The structure of PLAR_f filament exhibits a cross section with discontinuities and irregularities (Fig. 5a and b). The structure of the PLAR/CC_f filament appears slightly more homogenous, but still shows irregularities like the PLAR_f (Fig. 5c and d).

TG analysis performed on both filaments are reported in Fig. 6 and shows a negligible destabilization effect of charcoal on PLA toward decomposition reactions occurring only at temperature above 300 °C, higher than the temperature range used in the extrusion and FFF printing process.

The DSC curves of recycled filaments PLAR_f and PLAR/CC_f are reported in Fig. 7. As expected, the extrusion process causes a change in the molecular configuration, responsible of different properties of the filaments compared to the raw materials PLAW [29, 53]. In particular, glass transition and melting temperature (Fig. 7b, Table 5) were similar and lower than those of the raw materials (Fig. 4b). This may be due to the degradation of the materials during the extrusion process, caused by the processing conditions, i.e. temperature, shear stress, exposure to oxygen and moisture.

Finally, to further investigate the changes resulting from the addition of the filler to the recycled polymer matrix, GPC analyses were also performed on the produced filaments (Fig. 8, Table 6). Some of the authors [29] have already demonstrated that the PLA filament extruded (PLA_f, Table 6) starting from the neat PLA (PLA, Table 6) is affected by

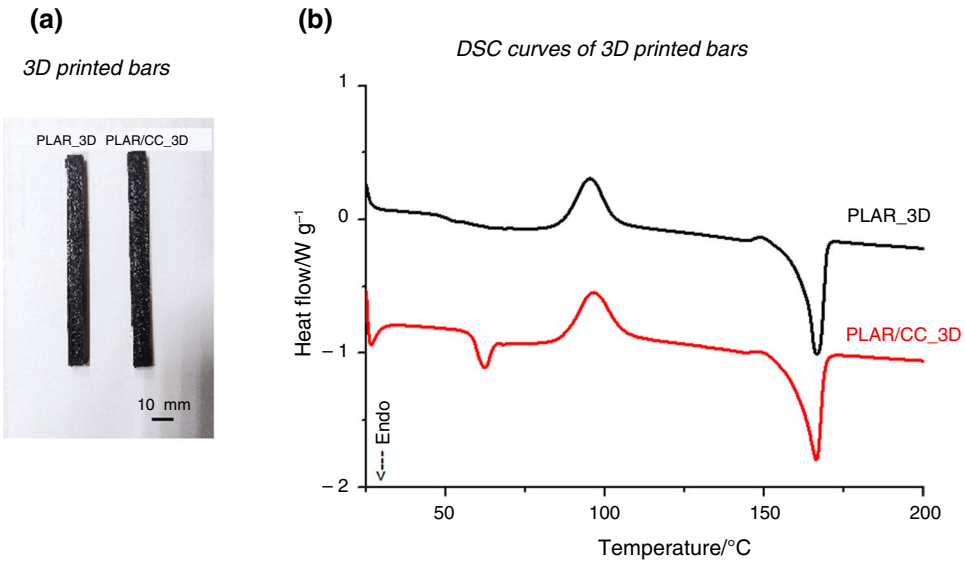

Fig. 10 **a** 3D printed bars; **b** DSC curves of 3D printed bars

chain scission, due to thermo-mechanical degradation and hydrolysis, occurring during polymer processing and related to high shear forces and temperatures and to residual water content, respectively [54]. These phenomena led to a reduction of the average molecular weights measured by GPC and equal to 106,418 KDa (M_n) and 209,921 KDa (M_w), for the neat PLA pellet to 58,569 KDa (M_n) and 142,096 KDa (M_w) for the filament extruded by the same neat PLA pellet. Recycling PLA from prints causes further degradation, resulting in an additional decrease in the length of the polymer chains (Fig. 8, Table 6). However, the GPC analysis of the filaments clearly confirms the stabilization effect of charcoal during the melt processing, according to a slight increase of the T_g measured by DSC of the filament containing CC (Table 5). Number averaged (M_n) and weight averaged (M_w) molecular weights of recycled PLA samples (PLAR_f and PLAR/CC_f), as derived by the GPC curves (Fig. 8) are shown in the Table 6.

Similarly, XRD measurements (Fig. 9) also reveal an effect of charcoal on the recycled PLA. The X-ray diffractogram of the pellet (sample PLA) shows a diffuse diffraction band from which a more defined peak emerges at $2\theta\ (^\circ) = 16.7^\circ$, assigned to the crystalline plane (110), as reported in the literature [29]. The X-ray diffractograms of the respective produced filament PLA_f and the recycled filament PLAR_f shows an increase in the amorphous band; in contrast PLAR/CC_f retains a certain degree of crystallinity even after extrusion, as can be seen from the peak at 16.7°.

Table 7 Thermal properties obtained from DSC analysis of 3D printed bars: glass transition temperature (T_g), temperature and enthalpy of crystallization (T_c and ΔH_c) and melting temperature and enthalpy (T_m and ΔH_m)

Sample	T_g /°C	T_c /°C	ΔH_c /J g^{-1}	T_m /°C	ΔH_m /J g^{-1}
PLAR_3D	56.6	95.2	24.8	166.1	32.4
PLAR/CC_3D	59.7	96.2	30.0	166.0	33.9

Characterization of 3D printed bars

DSC analysis performed on the 3D printed bars (PLAR_3D and PLAR/CC_3D) shows no significant variations between the thermal properties of the extruded filaments (subjected to two melting/solidification cycles) (Fig. 7b) and their corresponding 3D printed samples (subjected to three melting/solidification cycles) (Fig. 10b). The enthalpic relaxation peak is normally associated with the time the material was held at a temperature close to but below the glass transition temperature. The difference between the two DSC curves in Fig. 7 and in Fig. 10 is due to uncontrolled cooling conditions at the exit of the extruder die. The PLAR/CC_f sample cooled down very slowly below T_g after quenching.Thus, the re-extrusion process does not cause major changes in structure. However, this last melting solidification cycle is performed in the extruder of the 3D printing machine which is not equipped with a screw responsible of high shear rates as in filament production. Moreover, 3D printing is a fast process, so the polymer is kept at the molten state for a very short time (Table 7).

Nevertheless, the printability of PLA following the addition of charcoal improves considerably. This phenomenon is particularly visible from the results of flexural tests conducted on the 3D printed bars, in accordance with the ISO178 (2014) standard (Fig. 11). Flexural modulus of elasticity and strength, reported in Fig. 11a and b are higher for filled specimens. This results from the more defect-rich structure of PLAW_3D specimens as shown by the optical

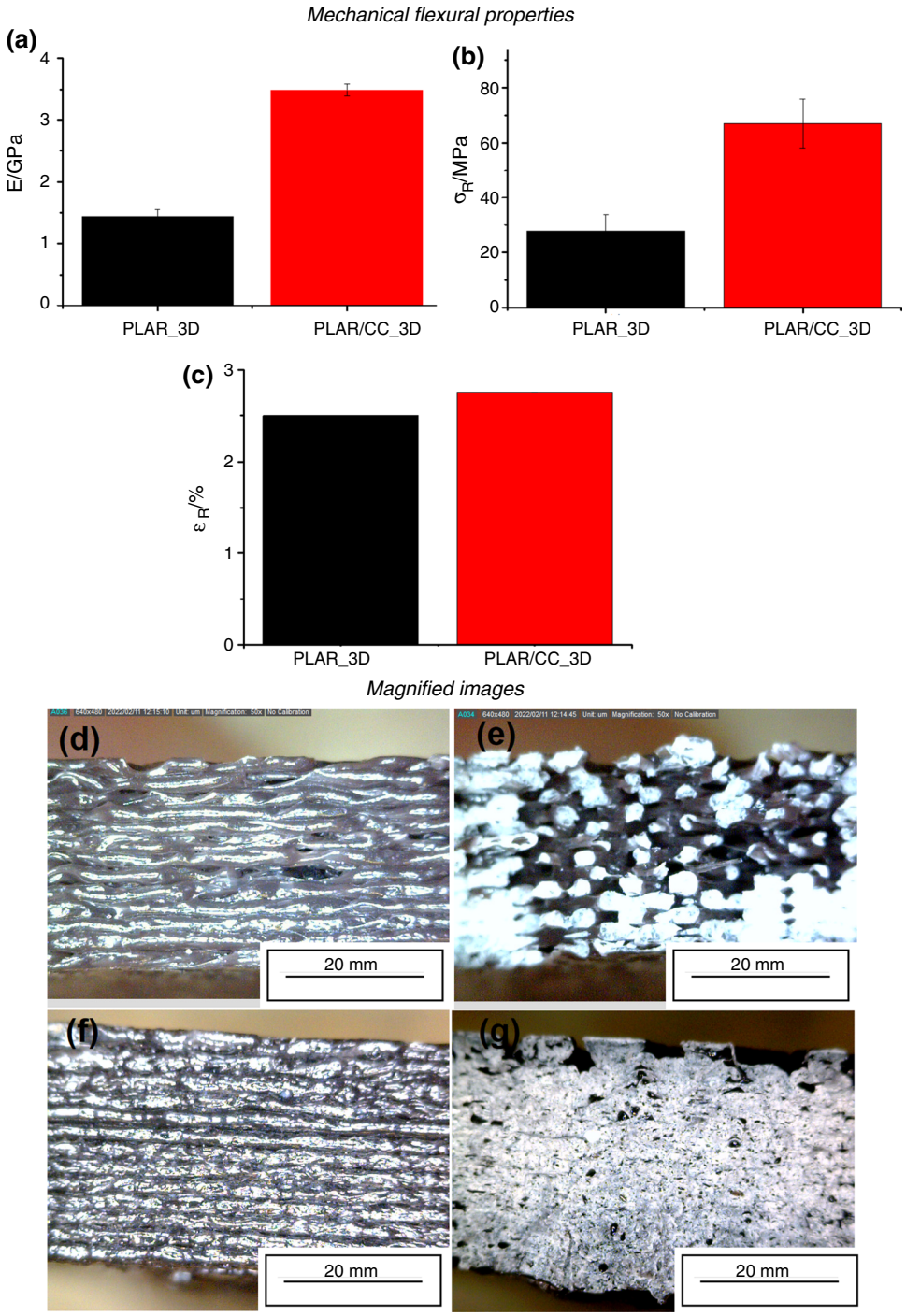

Fig. 11 Mechanical flexural properties of 3D printed bars: **a** flexural modulus of elasticity (GPa), **b** flexural stress (MPa), **c** flexural strain (%); Magnified images (50x) of the 3D printed bars: **d** PLAR_3D printing surface and **e** breaking surface after bending; **f** PLAR/CC_3D printing surface and **g** breaking surface after bending

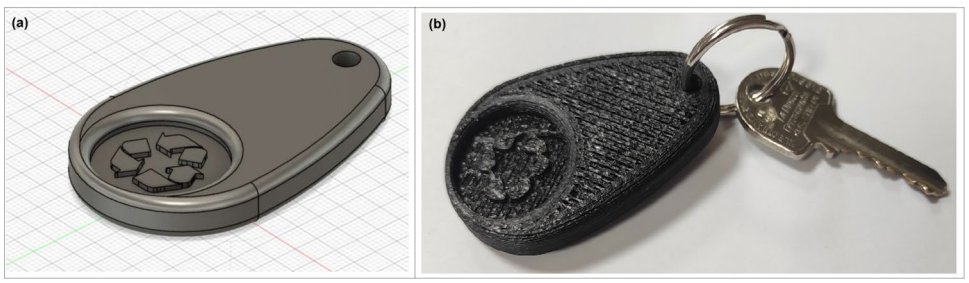

Fig. 12 **a** CAD model and **b** representative sample 3D printed from PLAR/CC_f filament

images of Fig. 11d–g. The images show good adhesion between the printed layers in the PLAR/CC_3D (Fig. 11f and g), unlike the PLAR_3D (Fig. 11d and e). Although defects are also present in PLAR/CC_3D, only moderately affect its mechanical properties. Overall, charcoal acts as a PLA melt stabilizer (to thermal–mechanical and hydrolytic degradation) during material extrusion, either for filament production either during FFF, increasing the printability and final properties of the recycled polymer.

All the scientific results obtained from this study confirm the stabilizing effect of charcoal during the melting process of recycled PLA. Indeed, without the presence of charcoal, it was only possible to print very simple shapes, as the bars used for the mechanical characterization, reported in Fig. 11. Instead, the presence of charcoal allowed the printability of less basic shapes with precision, as demonstrated by the representative sample (keyring) printed by FFF, using PLAR/CC_f filament (Fig. 12).

Conclusions

This paper proposes a sustainable method for the recycling and reuse of poly(lactic acid) (PLA), the most widely used thermoplastic material in Fused Filament Fabrication (FFF) printing. In order to limit the decrease properties of 3D printed models (made of recycled PLA) 2.5% wt. of charcoal (CC) was added to the recycled PLA matrix. The effect of the presence of small amount of CC on the melt stabilization of recycled PLA was, then, investigated by using several experimental techniques. In details, a complete characterization of the raw materials, of the produced filaments for FFF, and of the 3D-printed specimens used for mechanical properties, was carried out, by means of various analysis techniques (microscopy, elemental analysis, molecular analysis, DSC and TGA analysis, GPC analysis and bending tests). Thermal analysis shows that a good melt stabilization of the polymeric matrix is achieved by the addition of small concentrations of charcoal, within the range of temperatures that are usually used for filament extrusion and 3D printing. This effect is also visible from the results of the GPC analysis, which highlight a higher molecular weight of the recycled PLA containing CC and from the improvement of the mechanical properties of the composite 3D printed bars. The increased printability of the bio-composite filament containing CC is, finally, confirmed by the possibility to use it for the realization of a 3D printed model with a less simple form, compared to that obtained by using the recycled filament without the natural filler.

Funding Open access funding provided by Università del Salento within the CRUI-CARE Agreement.

References

1. Mikula K, Skrzypczak D, Izydorczyk G, Warchoł J, Moustakas K, Chojnacka K, et al. 3D printing filament as a second life of waste plastics—a review. Environ Sci Pollut Res. 2021;28:12321–33.
2. Wu H. Enhancements of sustainable plastics manufacturing through the proposed technologies of materials recycling and collection. Sustain Mater Technol. 2022;31:e00376. https://doi.org/10.1016/j.susmat.2021.e00376.
3. Patti A, Acierno D. Towards the sustainability of the plastic industry through biopolymers: properties and potential applications to the textiles world. Polymers (Basel). 2022;14:692.
4. Singh AV. Biopolymers in drug delivery: a review. Pharmacologyonline. 2011;1:666–74.
5. Galus S, Kibar EAA, Gniewosz M, Kraśniewska K. Novel materials in the preparation of edible films and coatings-a review. Coatings. 2020;10:1–14.
6. da Silva CJG, de Medeiros ADLM, de Amorim JDP, Nascimento HA, Converti A, Costa AFS, Sarubbo LA. Bacterial cellulose biotextiles for the future of sustainable fashion: a review. Environ Chem Lett. 2021;19:2967–80.
7. Ilyas RA, Sapuan SM, Harussani MM, Hakimi MYAY, Haziq MZM, Atikah MSN, et al. Polylactic acid (Pla) biocomposite: processing, additive manufacturing and advanced applications. Polymers. 2021;13(8):1326. https://doi.org/10.3390/polym13081326.
8. Ahmad MN, Ishak MR, Mohammad Taha M, Mustapha F, Leman Z, Anak Lukista DD, et al. Application of Taguchi method to optimize the parameter of fused deposition modeling (FDM) using oil palm fiber reinforced thermoplastic composites. Polymers (Basel). 2022;14:2140.
9. Udayakumar GP, Muthusamy S, BharathiSelvaganesh N, Sivarajasekar KR, Banat F, et al. Biopolymers and composites: properties, characterization and their applications in food, medical and pharmaceutical industries. J Environ Chem Eng. 2021;9(4):105322. https://doi.org/10.1016/j.jece.2021.105322S.
10 Shesan OJ, Stephen A C, Chioma AG, Neerish R, Rotimi SE. Improving the mechanical properties of natural fiber composites for structural and biomedical applications. In: Pereira AB, Fernandes FAO, editors. Renewable and sustainable composites. IntechOpen; 2019. https://doi.org/10.5772/intechopen.85252.
11 Khalid MY, Arif Z U. Novel biopolymer-based sustainable composites for food packaging applications: a narrative review. Food Packag Shelf Life. 2022;33:100892. https://doi.org/10.1016/j.fpsl.2022.100892.
12. Fico D, Rizzo D, Casciaro R, Esposito CC. A review of polymer-based materials for fused filament fabrication (FFF): focus on sustainability and recycled materials. Polymers (Basel). 2022;14:465. https://doi.org/10.3390/polym14030465
13 Medellin-Castillo HI, Zaragoza-Siqueiros J. Design and manufacturing strategies for fused deposition modelling in additive

manufacturing: a review. Chin J Mech Eng. 2019. https://doi.org/10.1186/s10033-019-0368-0.
14. Romani A, Rognoli V, Levi M. Design, materials, and extrusion-based additive manufacturing in circular economy contexts: from waste to new products. Sustain. 2021;13:1–23.
15 Kristiawan RB, Imaduddin F, Ariawan D, Ubaidillah ZA. A review on the fused deposition modeling (FDM) 3D printing: Filament processing, materials, and printing parameters. Open Eng. 2021;11(1):639–49. https://doi.org/10.1515/eng-2021-0063.
16. Shanmugam V, Pavan MV, Babu K, Karnan B. Fused deposition modeling based polymeric materials and their performance: a review. Polym Compos. 2021;42:5656–77.
17. Biswas MC. Fused deposition modeling 3D printing technology in textile and fashion industry: materials and innovation. Mod Concepts Mater Sci. 2019;2:1–5.
18 Schirmeister CG, Hees T, Licht EH, Mülhaupt R. 3D printing of high density polyethylene by fused filament fabrication. Addit Manuf. 2019;28:152–9. https://doi.org/10.1016/j.addma.2019.05.003.
19 Gao X, Qi S, Kuang X, Su Y, Li J, Wang D. Fused filament fabrication of polymer materials: A review of interlayer bond. Addit Manuf. 2021;37:101658. https://doi.org/10.1016/j.addma.2020.101658.
20. Pezzana L, Riccucci G, Spriano S, Battegazzore D, Sangermano M, Chiappone A. 3D printing of pdms-like polymer nanocomposites with enhanced thermal conductivity: boron nitride based photocuring system. Nanomaterials. 2021;11:1–17.
21. Corcione CE, Gervaso F, Scalera F, Montagna F, Maiullaro T, Sannino A, et al. 3D printing of hydroxyapatite polymer-based composites for bone tissue engineering. J Polym Eng. 2017;37:741–6. https://doi.org/10.1515/polyeng-2016-0194
22. Esposito Corcione C, Gervaso F, Scalera F, Padmanabhan SK, Madaghiele M, Montagna F, et al. Highly loaded hydroxyapatite microsphere/ PLA porous scaffolds obtained by fused deposition modelling. Ceram Int. 2019;45:2803–10. https://doi.org/10.1016/J.CERAMINT.2018.07.297
23. Bardot M, Schulz MD. Biodegradable poly(Lactic acid) nanocomposites for fused deposition modeling 3D printing. Nanomaterials. 2020;10:1–20.
24. Dul S, Fambri L, Pegoretti A. Development of new nanocomposites for 3D printing applications. Struct Prop Addit Manuf Polym Compon. 2020. https://doi.org/10.1016/B978-0-12-819535-2/00002-8.
25. Ye Q, Huang Z, Hao Y, Wang J, Yang X, Fan X. Kinetic study of thermal degradation of poly(l-lactide) filled with β-zeolite. J Therm Anal Calorim. 2016;124:1471–84.
26. Tao Y, Liu M, Han W, Li P. Waste office paper filled polylactic acid composite filaments for 3D printing. Compos Part B Eng. 2021;221:108998. https://doi.org/10.1016/j.compositesb.2021.108998.
27. Ahmad MN, Ishak MR, Taha MM, Mustapha F, Leman Z. Rheological properties of natural fiber reinforced thermoplastic composite for fused deposition modeling (FDM): a short review. J Adv Res Fluid Mech Therm Sci. 2022;98:157–64.
28. Fico D, Rizzo D, De Carolis V, Montagna F, Palumbo E, Corcione CE. Development and characterization of sustainable PLA/Olive wood waste composites for rehabilitation applications using fused filament fabrication (FFF). J Build Eng. 2022;56:104673. https://doi.org/10.1016/j.jobe.2022.104673.
29. Fico D, Rizzo D, De Carolis V, Montagna F, Esposito CC. Sustainable polymer composites manufacturing through 3D printing technologies by using recycled polymer and filler. Polymers (Basel). 2022;14:3756. https://doi.org/10.3390/polym14183756
30. Esposito Corcione C, Palumbo E, Masciullo A, Montagna F, Torricelli MC. Fused Deposition Modeling (FDM): an innovative technique aimed at reusing Lecce stone waste for industrial design and building applications. Constr Build Mater. 2018;158:276–84. https://doi.org/10.1016/j.conbuildmat.2017.10.011.
31. Cicala G, Saccullo G, Blanco I, Samal S, Battiato S, Dattilo S, et al. Polylactide/lignin blends: Effects of processing conditions on structure and thermo-mechanical properties. J Therm Anal Calorim. 2017;130:515–24.
32. Özmen U, Baba BO. Thermal characterization of chicken feather/PLA biocomposites. J Therm Anal Calorim. 2017;129:347–55.
33. Beltrán FR, Arrieta MP, Moreno E, Gaspar G, Muneta LM, Carrasco-Gallego R, et al. Evaluation of the technical viability of distributed mechanical recycling of PLA 3D printing wastes. Polymers. 2021;12:1247.
34. Muñoz VG, Muneta LM, Carrasco-Gallego R, Marquez JDJ, Hidalgo-Carvajal D. Evaluation of the circularity of recycled PLA filaments for 3D printers. Appl Sci. 2020;10:8967.
35 Balla E, Daniilidis V, Karlioti G, Kalamas T, Stefanidou M, Bikiaris ND, et al. Poly(lactic acid): a versatile biobased polymer for the future with multifunctional properties applications. Polymers (Basel). 2021;13:1822.
36. Algarni M, Ghazali S. Comparative study of the sensitivity of pla, abs, peek, and petg's mechanical properties to fdm printing process parameters. Crystals. 2021;11:995.
37. Ibrahim NI, Shahar FS, Sultan MTH, Md Shan AU, Safri SNA, Yazik MHM. Overview of bioplastic introduction and its applications in product packaging. Coatings. 2021;11:1423.
38. Zhao X, Cornish K, Vodovotz Y. Narrowing the gap for bioplastic use in food packaging: an update. Environ Sci Technol. 2020;54:4712–32.
39. Murariu M, Paint Y, Murariu O, Laoutid F, Dubois P. Recent advances in production of ecofriendly polylactide (PLA)–calcium sulfate (anhydrite II) composites: from the evidence of filler stability to the effects of PLA matrix and filling on key properties. Polymers (Basel). 2022;14:2360.
40 Jalali A, Huneault MA, Elkoun S. Effect of molecular weight on the nucleation efficiency of poly(lactic acid) crystalline phases. J Polym Res. 2017. https://doi.org/10.1007/s10965-017-1337-x.
41 Anderson I. Mechanical properties of specimens 3D printed with virgin and recycled polylactic acid. 3D Print Addit Manuf. 2017;4:110–5.
42 Lanzotti A, Martorelli M, Maietta S, Gerbino S, Penta F, Gloria A. A comparison between mechanical of specimens 3D printed with virgin and properties recycled PLA. Sci Direct. 2019;79:143–6. https://doi.org/10.1016/j.procir.2019.02.030.
43. Zhao P, Rao C, Gu F, Sharmin N, Fu J. Close-looped recycling of polylactic acid used in 3D printing: An experimental investigation and life cycle assessment. J Clean Prod. 2018;197:1046–55.
44. Grigora ME, Terzopoulou Z, Tsongas K, Klonos P, Kalafatakis N, Bikiaris DN, et al. Influence of reactive chain extension on the properties of 3d printed poly(Lactic acid) constructs. Polymers (Basel). 2021;13:1–18.
45. D'Urso L, Acocella MR, Guerra G, Iozzino V, De Santis F, Pantani R. PLA melt stabilization by high-surface-area graphite and carbon black. Polymers (Basel). 2018;10:1–13.
46 D'Urso L, Acocella MR, De Santis F, Guerra G, Pantani R. Poly(L-lactic acid) nucleation by alkylated carbon black. Polymer. 2022;256:125237.

47. Kiani A, Acocella MR, Granata V, Mazzotta E, Malitesta C, Guerra G. Green oxidation of carbon black by dry ball milling. ACS Sustain Chem Eng. 2022. https://doi.org/10.1021/acssuschemeng.2c05638.
48. Acocella MR, Maggio M, Ambrosio C, Aprea N, Guerra G. Oxidized carbon black as an activator of transesterification reactions under solvent-free conditions. ACS Omega. 2017;2:7862–7.
49 Di Ruocco C, Acocella MR, Guerra G. Release of cationic drugs from charcoal. Materials (Basel). 2019;12:683.
50. Reignier J, Tatibouet J, Gendron R. Effect of dissolved carbon dioxide on the glass transition and crystallization of poly(lactic acid) as probed by ultrasonic measurements. J Appl Polym Sci. 2009;112:1345–55.
51. Chen X, Kalish J, Hsu SL. Structure evolution of α-phase Poly(lactic acid). J Polym Sci Part B Polym Phys. 2011;49:1446–54.
52. Stagnaro P, Luciano G, Utzeri R. La calorimetria differenziale a scansione e l'analisi termogravimetrica nella caratterizzazione termica dei materiali polimerici. 73–98
53. Carrasco F, Pagès P, Gámez-Pérez J, Santana OO, Maspoch ML. Processing of poly(lactic acid): characterization of chemical structure, thermal stability and mechanical properties. Polym Degrad Stab. 2010;95:116–25.
54 Cruz FA, Sanchez HB, Hoppe S, Camargo M. Polymer recycling in an open-source additive manufacturing context: mechanical issues. AddIT Manuf. 2017;17:87–105. https://doi.org/10.1016/j.addma.2017.05.013.